Biophysical analysis of lipidic nanoparticles.

Annaïg J. Rozo*[1], Megan H. Cox*[1,2], Andrew Devitt[1], Alice J. Rothnie[1] and Alan D. Goddard[1†]

*These authors contributed equally to this work.

[1] School of Life and Health Sciences, Aston University, Birmingham, B4 7ET, UK.

[2] Meritics Ltd., Unit 3, Clipstone Brook Industrial Estate, Cherrycourt Way, Leighton Buzzard, LU7 4GP

[†] Corresponding author a.goddard@aston.ac.uk

Highlights

- **Biological nanoparticles play key roles in research and therapeutics.**
- **A range of techniques are available to study such particles in terms of size and concentration.**
- **Each technique has associated advantages and disadvantages.**
- **Novel approaches allow the analysis of the full range of nanoparticles with a single instrument.**

Abstract

Biological nanoparticles include liposomes, extracellular vesicle and lipid-based discoidal systems. When studying such particles, there are several key parameters of interest, including particle size and concentration. Measuring these characteristics can be of particular importance in the research laboratory or when producing such particles as biotherapeutics. This article briefly describes the major types of lipid-containing nanoparticles and the techniques that can be used to study them. Such methodologies include electron microscopy, atomic force microscopy, dynamic light scattering, nanoparticle tracking analysis, flow cytometry, tunable resistive pulse sensing and microfluidic resistive pulse sensing. Whilst no technique is perfect for the analysis of all nanoparticles, this article provides advantages and disadvantages of each, highlighting the latest developments in the field. Finally, we demonstrate the use of microfluidic resistive pulse sensing for the analysis of biological nanoparticles.

Keywords: Nanoparticle, MPRS, nCS1, Extracellular vesicles, Liposomes

List of abbreviations

ACdEV	Apoptotic Cell-Derived Extracellular Vesicle
AFM	Atomic Force Microscopy
An-V	Annexin V
API	Active Pharmaceutical Ingredient
BSA	Bovine Serum Albumin
CCD	Charged-Coupled Device
CSD	Concentration Size Distribution
DDS	Drug Delivery System
DLS	Dynamic Light Scattering
EM	Electron Microscopy
ET	Electron Tomography
EV	Extracellular Vesicle
FCM	Flow Cytometry
FSC	Forward Scatter
HRFCM	High-Resolution Flow Cytometry

HRTEM	High-Resolution Transmission Electron Microscopy
IC	Intracellular Communication
LET	Liposomal Encapsulation Technology
MRPS	Microfluidic Resistive Pulse Sensing
MSP	Membrane Scaffold Protein
MVB	Multivesicular Body
NP	Nanoparticle
NTA	Nanoparticle Tracking Analyser
PS	Phosphatidylserine
PZT	Piezoelectric
RI	Refractive Index
RPS	Repulsive Pulse Sensing
SEM	Scanning Electron Microscopy
SFM	Scanning Force Microscopy
SIOS	Scanning Ion Occlusion Spectroscopy
SMALP	Styrene Maleic Acid Lipid Particle
SSC	Side Scatter
TDFM	Transverse Dynamic Force Microscopy
TEM	Transmission Electron Microscopy
TRPS	Tunable Resistive Pulse Sensing
UC	Ultra-Centrifugation
3-D	3-Dimensional

Introduction

Nanoparticles

Nanoparticle (NP) is a term which encompasses several subpopulations. Nanoparticles can be naturally occurring, for example, extracellular vesicles (EVs) released by cells across the three main groups of the phylogenetic tree: Archaea, Bacteria and Eukarya. They can also be engineered, as with viruses used for vaccines; they can be biological (for example liposomes) or non-biological (such as metal or metal-derived NPs) or a combination of both. They could also be accidental in their production, such as exhaust fumes. In this review, we will use the term "nanoparticle" to refer to extracellular vesicles, liposomes and nanodisc systems, e.g. styrene maleic acid lipid particles (SMALPs).

Whilst the international standards organisation (ISO)[1] defines nanoparticles as ranging in size from 1 to 100nm, it is generally accepted that biological nanoparticles may be larger than this within the sub-micron range. Due to their size, NPs have a larger surface area to volume ratio when compared to bulk materials, which give them interesting physical properties. Their size and composition can make them challenging to study experimentally.

Extracellular vesicles

Extracellular vesicles (EVs) are membrane-surrounded structures released by healthy, apoptotic and diseased cells. They were first described in 1967 by P. Wolf [2] and are found in most biological fluids. They are a highly heterogeneous population which vary in size, content, and mechanism of formation [3]. Their origin can also be used to classify them further. The field acknowledges three distinct subpopulations: apoptotic vesicles (30nm-5μm), microvesicles (100nm-1μm) and exosomes (30nm-100nm) (Figure 1). Exosomes are initially formed inside multivesicular bodies (MVBs) and are further released through exocytosis into the extracellular environment. Alternatively, microvesicles and apoptotic bodies are produced through budding of the plasma membrane.

Apoptotic cell-derived EVs (ACdEVs) encompass apoptotic bodies, apoptotic microvesicles and exosome-like vesicles. Evidence suggests that ACdEV biogenesis seems to be more complex as they can be formed through membrane protrusions termed apoptopodia [4], or through plasma membrane blebbing as mentioned previously. However, as little is reported in the literature regarding ACdEVs, other novel mechanisms of biogenesis are worth investigating.

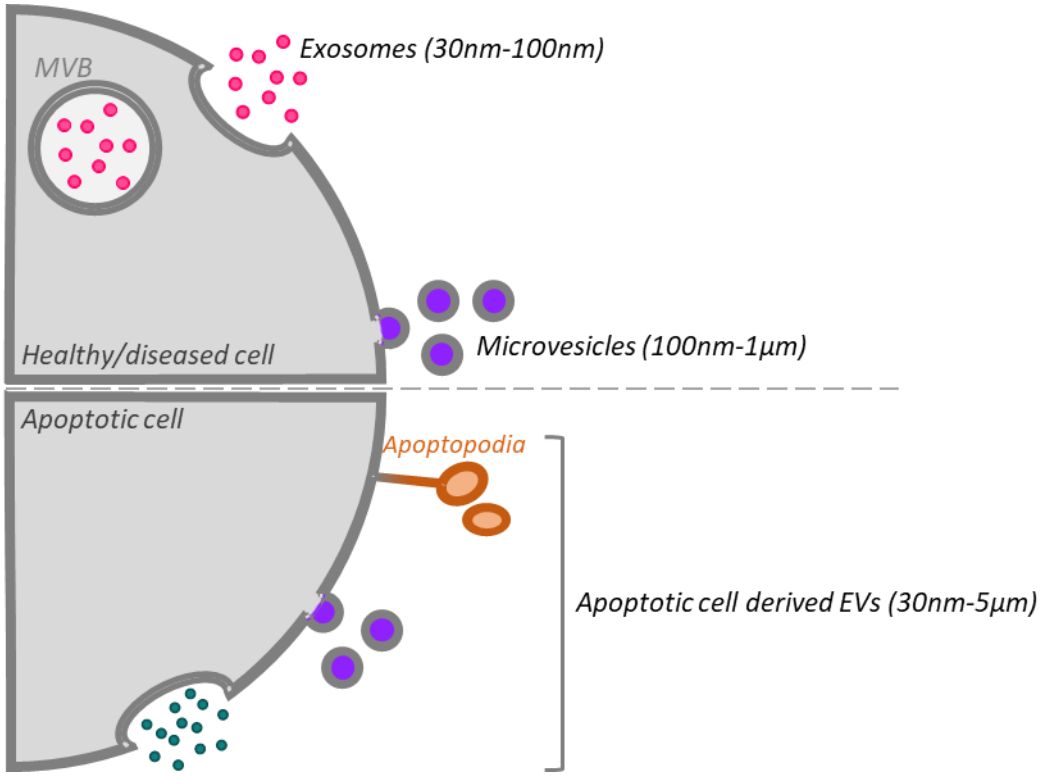

Figure 1 Extracellular vesicles formation and different subpopulations. *Healthy and diseased cells release two mains forms of EVs named exosomes and microvesicles. They are released through the exocytosis of multivesicular bodies (MVBs) and via plasma membrane shedding. Apoptotic cells release ACdEVs of various size through membrane protrusion, membrane blebbing and other mechanisms. Green vesicles represent exosome-like ACdEVs.*

It was first believed that EVs were cellular debris, but subsequent research has shown they contain a specific subset of proteins, mRNAs, miRNAs, and lipids rather than random cellular components [5]. It has been demonstrated that EVs play a major pathophysiological role in various biological process (apoptotic cell clearance, infection, immune response, antigen presentation [6]). They function to transport and deliver cargo molecules between cells [7]. This EV-mediated intercellular communication (IC) exists in healthy tissues and when altered, can lead to a variety of diseases, namely autoimmune diseases and cancer. In the past few decades, EVs have received a great deal of interest for their diagnostic and therapeutic potential [8].

Liposomes

Liposomes were first discovered by Bangham and his co-workers in 1961 [9], and can be described as spherical artificial vesicles of various lamellarity: usually one or two phospholipid bilayers. Liposomes are formed spontaneously, but many different methods of preparation exist. These can be divided between passive or active loading techniques. The most common passive techniques are mechanical dispersion, solvent dispersion or detergent removal, such as sonication and extrusion [10]. Similar structures can also be formed from polymers (sometimes referred to as polymersomes) [11].

Conventional liposomes are commonly made of ester phospholipids such as phosphatidylcholine. A new generation of liposomes have modified formulations in order to try to overcome instability issues and enhance specificity [12]. For example, archeasomes contain one or more lipids found in archeobacterial membranes that offer higher stability because of di-ether linkages [13]. Additionally, virosomes are a combination of liposomes with virus-derived envelope proteins, allowing the fusion

of the virosomes with the target cell [14]. Finally, novasomes are paucimellar vesicles formed of two to seven bilayer membranes commonly used in cosmetics [15].

Liposomes can be loaded with different drugs and or molecules and used as drug carriers to deliver a range of active pharmaceutical ingredients (API) to a site of action for therapeutic and diagnostic purposes [16]. This liposomal encapsulation technology (LET) can involve drug molecules, gene therapies and bioactive agents. Hydrophobic API can be incorporated into the phospholipid bilayers, whereas hydrophilic API can be encapsulated inside the aqueous centre. LET has been shown to increase the stability and decrease the toxicity of the active molecules making it more efficient [17]. Different types of liposomal drug delivery system (DDS) exist [18], for example, by coupling the liposomes to targeting ligands to increase the specificity. These carriers are most valuable because of their biocompatibility and non-immunogenicity [19].

Another use for liposomes is their relevance as a biological model [20],[21]. They can be used to mimic both extracellular vesicles and cells, offering a non-invasive alternative to study biological processes and test drugs. Their composition, size and charge can be tuned to make a highly accurate model.

Disc systems

In membrane protein research, proteins often have to be isolated from the membrane in order to study them. This has often resulted in the use of detergents to solubilise the membrane, and therefore the protein, into detergent micelles. Throughout the past decades, it has become more apparent the native lipid environment surrounding the protein plays numerous roles in the structural stability and functionality of the protein. Hence, alternatives to detergents are advantageous [22].

Membrane scaffold proteins (MSPs) are one of the alternatives to a purely detergent-based isolation system. Bayburt et al., 2002 [24] first described the formation of bilayer patches surrounded and stabilised by a ring of amphipathic helical protein, termed membrane scaffold proteins. The process of forming these patches was described as a self-assembly mechanism whereby lipids, MSPs, and detergent were added to protein-detergent micelles forming particles of around 10nm in size [25] (Figure 2).

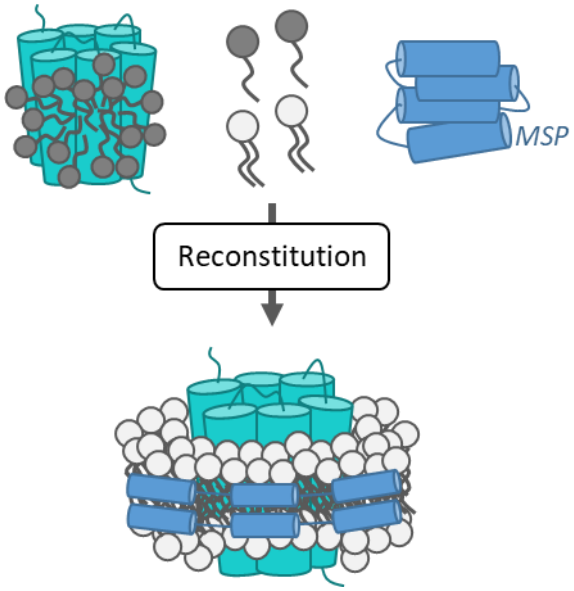

Figure 2 Schematic demonstrating the formation of MSP nanodiscs*. A protein is isolated from the membrane via detergent solubilisation. A mixture of lipids and membrane scaffold proteins (MSPs) are added to the protein-detergent micelle solution, this results in the self-assembly of MPS encapsulated protein-lipid nanodiscs.*

A more recent approach is the use of styrene-maleic acid (SMA) copolymers and derivatives to isolate membrane proteins in a nanometer-sized disc, known as SMA lipid particles (SMALPs) (Figure 3). The technique was first described in 2009 by Knowles *et al.* [26] and has the distinct advantage that the protein is extracted directly from the membrane without the need for detergent, and therefore maintains a near-native lipid environment, which is beneficial for downstream research [26].

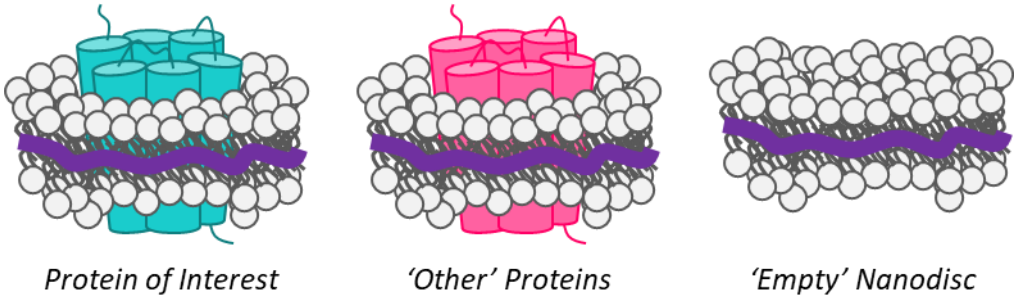

Figure 3 Schematic of SMALP encapsulated nanodiscs*. SMA copolymers punch holes in the membrane encapsulating anything that is present, i.e. membrane proteins (protein of interest as well as other proteins) or 'empty' lipid only discs.*

The greatest challenge of single NP based isolation and analysis is still the size of the NPs, which are below the reach of conventional detection methods [27]. In this review, we will present the main methods for NP analysis and their limitations, focusing on single particle-based quantification and size profiling. Finally, an advancement in NP analysing technology will be introduced as an alternative to study NPs with preliminary data presented.

Conventional methods for NP analysis

Common isolation methods for NPs include; ultracentrifugation (UC) and precipitation alongside size-, immunoaffinity capture-, and microfluidic-based techniques [28]. Microfluidic isolation is a promising field, which offers miniaturisation of conventional techniques, quicker purification times and improved resolution while enabling a continuous separation of the NPs. Following isolation using any approach, it is often desirable to analyse the size of the NPs to ensure either efficient separation or to define the nature of the sample.

Electron microscopy (EM)

Conventional optical microscopes cannot be used due to NPs being below the diffraction limit of visible light (200nm). Traditionally, the only way to visualise NPs via microscopy is by using the shorter wavelength and higher frequency of an electron microscope. As the wavelength of an electron can be up to 100,000 times shorter than that of visible light photons, electron microscopes have a higher resolving power that can reveal the structure of smaller objects, i.e. in the nanoscale. The first electron microscope was built in 1931 by Ruska and Knoll. Nowadays, two types of electron microscopes exist Scanning EM (SEM) and Transmission EM (TEM) (Figure 4).

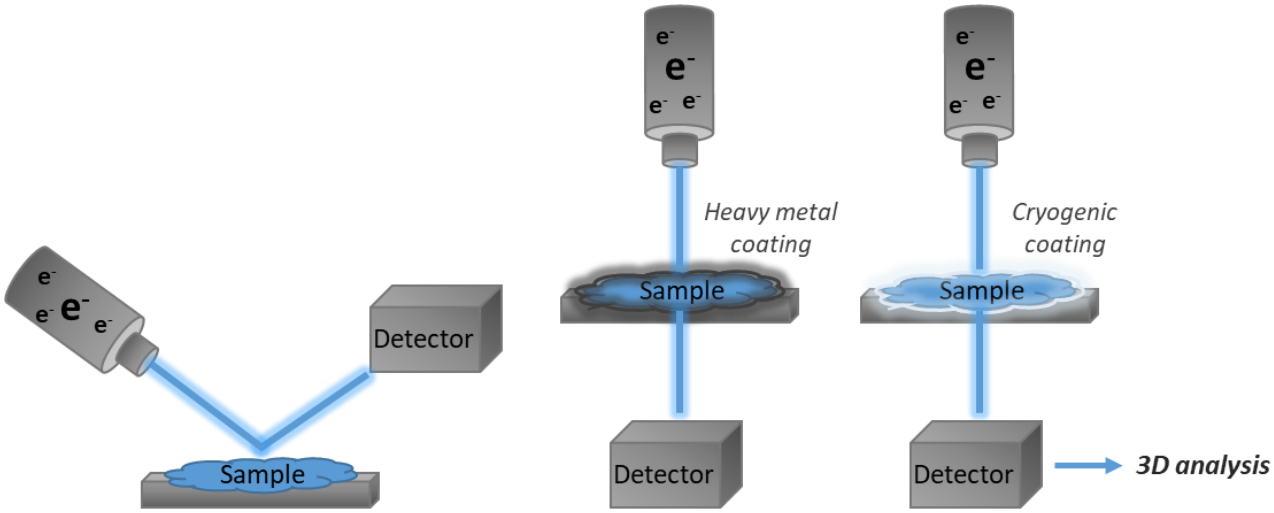

Figure 4 Simple schematic of the most common EM techniques. *Scanning electron microscopy determines information about the sample surface. Transmission electron microscopy sends electrons through the heavy metal coated sample, acquiring structural information. Cryo-transmission electron microscopy utilises freezing of the sample to retain native structural information.*

SEM is an electrical conductivity-based EM where the electron beam is focused onto the surface of the samples, scanning it line by line. A detector simultaneously counts the scattered secondary electrons. The images acquired by SEM only allow visualisation of the surface of the specimen, but SEM can also provide 3-dimensional (3D) images. However, this method offers a lower resolution than TEM [29].

TEM is an electron emission-based EM for thin samples (~100nm). Here, the beam of accelerated electrons passes through the samples. The detector is below the sample retrieving the electron to provide structural information. The entire electron path through the column must be under vacuum. High-resolution TEM (HRTEM) is now able to provide a resolution below 0.5 angstroms [30]. However, this resolution is limited to non-biological samples, regarding lipidic nanoparticles the resolution of ~1.5 angstroms is more accurate [31].TEM can have variants such as immune-EM, Cryo-EM (single-particle and tomography), 3D-EM and conventional TEM.

For conventional TEM, the thin sections are coated with heavy metals in order to obtain a better contrast and to visualise the lipid bilayer [32]. Depending on where the section was made, the diameter can differ. The morphology of the whole particle thus remains uncertain. Fixatives can be added to improve the sample retention. This method is a rapid way of confirming the presence of NPs in a sample.

The least invasive technique is cryo-TEM, where the sample is frozen using a cryogen (liquid ethane or propane) (Figure 4). Upon rapid freezing, a thin liquid film of the buffer is transformed into an amorphous solid, allowing the object beneath to be observed in the native frozen-hydrated state. The immediate freezing of the sample allows no time for crystal formation, removing the need to use fixative and heavy metals. The sample is then transferred in a cryo-electron microscope and observed at low temperature (-170 °C). The lipid bilayer appears as two thin dark lines because of the phosphorous atoms (the heaviest) scattering more electrons [33].

Phenotyping of EVs can be performed using cryo-TEM combined with immune-gold-labelling. Gold particles provide high contrast in EM thanks to their large electron scattering properties (i.e. plasma EVs exposing phosphatidylserine (PS) labelled with annexin V (An-V) conjugated with gold particles) [34]. Additionally, electron tomography (ET) can be used for 3D reconstruction based on 2-dimensional pictures taken at many different angles creating a tilt series. This can be combined with cryo-TEM by creating electronic slices as thin as 1nm through the reconstructed 3-D volume [35]. The details are much finer compared to cryo-EM alone and allow discrimination of vesicles spatially below or inside another one. The angles of the image do not yet permit a fully 3D structure due to an artefact that is referred to in the literature as "the missing wedge" [28, 29].

TEM has some potential disadvantages for particle analysis including possible radiation damage to the sample such as re-conformation and de-crystallisation to the breaking of atom bonds, removal of side-chains and in general a loss of mass [38].

Atomic force microscopy (AFM)

Atomic force microscopy (AFM) is a type of scanning force microscopy (SFM) developed in the 1980s by Binning, Quate, and Gerber [39]. Typically, a near-horizontal cantilever is used with a "nanofiber" tip facing towards the sample. Lasers are then reflected off the back of the cantilever to track the change in its displacement, which depending on its mode of operation, provides different information (Figure 5).

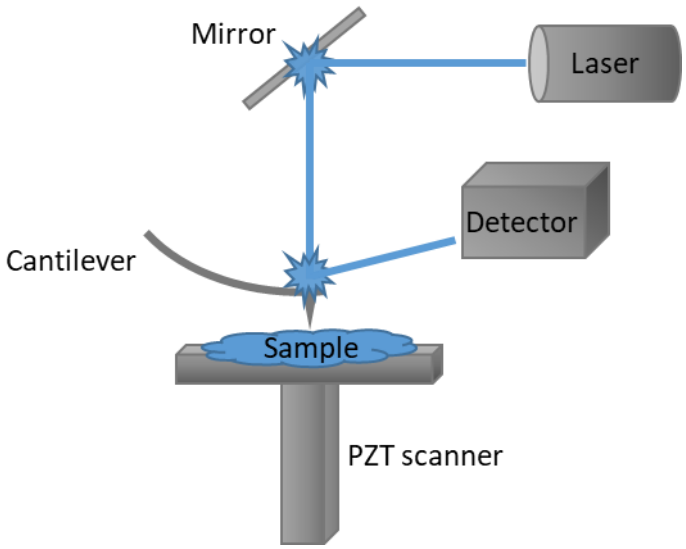

Figure 5 Schematic representation of Atomic Force Microscopy. *The cantilever is in contact with the sample and the sample stage (piezoelectric (PZT) scanner) moves the x, y, and z position. A laser monitors the position of tip with feedback via a photodiode to the piezoelectric scanner to move the stage z-position to build a topological image at atomic resolution.*

There are three modes of AFM; the first mode is contact-based, where the sample stage is positioned to provide a small upwards deflection of the tip when contact occurs. The sample is then moved along the x- and y-axis. As the topology of the sample changes so does the level of cantilever deflection, some operate by simply tracking the height of the cantilever in absolute terms and generating the topology from this [40]. In others, the system will for each x and y co-ordinate aim to deliver a consistent level of deflection, and the required changes in the samples z position will generate the topological map.

The second mode is non-contact. Here instead of an upwards deflection, a downwards deflection is observed. This is due to atomic forces, e.g. Van der Waals on this scale interacting with the cantilever, pulling it towards the sample [41]. Again, the concept is to maintain a consistent deflection and generate a topological map through record stage positioning.

There is a third non-contact mode. This involves the cantilever being oscillated at very high frequencies. As the tip gets close to the sample, either atomic forces or physical interactions, often with a layer of moisture present, leads to a dampening of the oscillation frequency. A consistent level of damping is required to generate the topological map [42].

Some advantages are that AFM can be operated in ambient conditions and often requires no special preparation of the sample. The sample sizes are often small, e.g. <200nm squared. Advances in piezoelectrics and control systems allow for near real-time scanning to generate videos, particularly useful for studying biological samples [43],[44]. Improved methods are always being developed, e.g. Transverse dynamic force microscopy (TDFM) which uses a vertical cantilever [45].

Dynamic light scattering (DLS)

Dynamic light scattering (DLS) is one of the most common and simple techniques used in the analysis of particle size distribution [46]. DLS is a measure of time-dependent fluctuations in the scattered light of particles undergoing Brownian motion (diffusion caused by random collisions with solvent molecules). A particle's hydrodynamic diameter is calculated as a function of the diffusion coefficient. Where the diffusion coefficient is inversely proportional to the particle size according to the Stokes-Einstein equation (Figure 6). This calculation assumes that all particles are spherical, reporting an equivalent particle diameter which can be disadvantageous for studying discoidal systems.

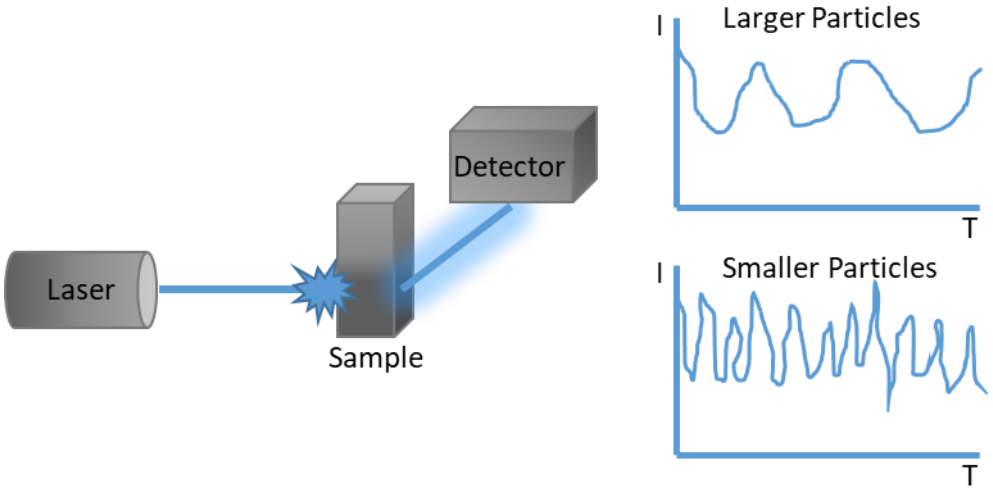

Figure 6 Schematic of Particle Size Analysis by Dynamic Light Scattering. *A laser illuminates particles undergoing Brownian motion in a sample. A photodetector measures the fluctuations in the intensity of scattered light over a time period. Stokes-Einstein's equation is used to calculate the hydrodynamic diameter of the particles.*

DLS can analyse particles ranging from 0.5 to 10,000nm dependent on the instrument and can analyse as little as 45µL of the sample, although common practice is to use a standard size cuvette which requires around 500µL for analysis. DLS also uses Rayleigh's approximation, where the intensity, I, of scattered light is proportional to the sixth power of the particle diameter, d: $I \propto d^6$ (i.e. a particle of 100nm will scatter light with a million times the intensity of a 10nm particle)[46],[47]. This means that

DLS has an inherent bias towards larger particles and therefore, a tendency to oversize particles in a polydisperse mixture and as such, it is not suitable for highly polydisperse samples.

Nanoparticle tracking analyser (NTA)

Nanoparticle tracking analysis (NTA) can be used for various applications, including but not limited to vesicles, exosomes, and proteins [48]. NTA uses the same underlying principle as DLS as it measures time-dependent fluctuations in scattered laser light of particles undergoing Brownian motion to determine their hydrodynamic radius. Where NTA differs is how it detects the scattered light. NTA uses a laser beam to illuminate particles, and the scattered light is easily visualised with a conventional microscope equipped with a 20x objective lens. Particle movement, i.e. scattered light, is then recorded with a light-sensitive charged-coupled device (CCD) or CMOS camera, arranged at a 90° angle to the irradiation plane [49]. The camera operates at 30 frames per second (fps), capturing a video file of the particles moving under Brownian motion. The software tracks many particles individually and using the Stokes-Einstein equation calculates their hydrodynamic diameters (Figure 7) [50]. As NTA is capable of tracking individual particles, the concentration of particles within a sample can be calculated. However, this requires calibration with standards of a known size and concentration.

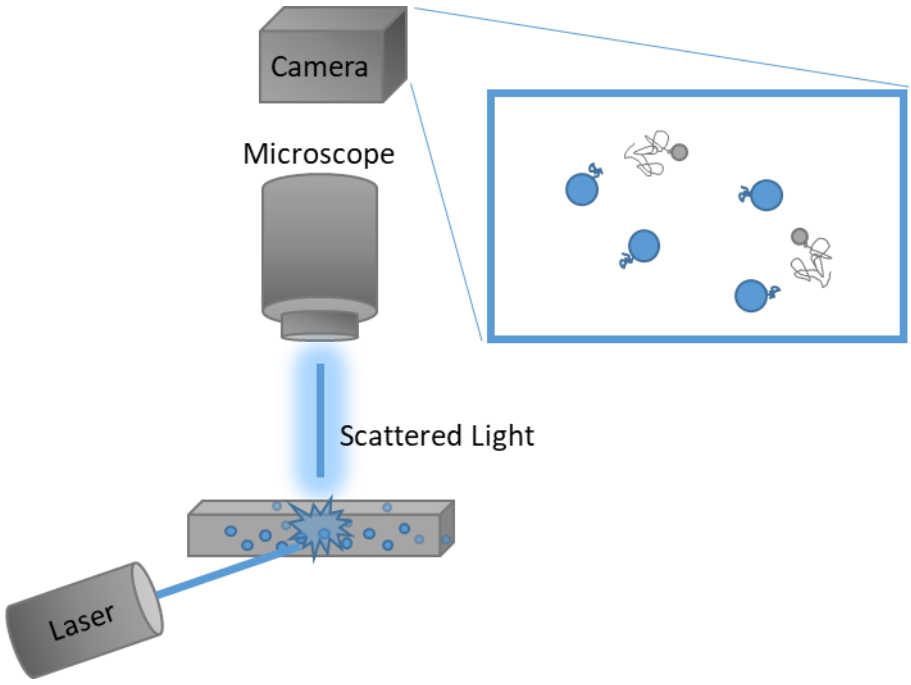

Figure 7 Schematic Representation of Particle Size Analysis by Nanoparticle Tracking Analysis. *A laser illuminates particles undergoing Brownian motion in a sample. Particle movement i.e. scattered light is then recorded with a light-sensitive charged-coupled device (CCD) or CMOS camera. Software tracks individual particles and uses the Stokes-Einstein equation calculates their hydrodynamic diameters.*

NTA is reported to size particles between 10 and 1000nm at a concentration range of 1E+06 to 1E+09 particles.mL^{-1}; however, this is sample and system configuration dependent [50]. For samples (such as EVs), where the refractive index (RI) of the particle is close to the RI of the electrolyte it is suspended in, the detection resolution is compromised, resulting in a restricted size analysis range and unreliable

concentration determination [51]. Like DLS, NTA also has restricted resolution for polydisperse samples due to Rayleigh's approximation, making it difficult to detect and track small particles [46].

Conventional Flow Cytometry (FCM)

Flow cytometry (FCM) is a laser-based technology developed for high throughput, multiparametric analysis of individual particles (e.g. cells). It allows the analysis of thousands of cells per second. However, in order to be detected, particles need to scatter light and/or induce fluorescence. NPs are much smaller than the cells for which flow cytometry was designed. Conventional FCM has a lower detection limit for polystyrene beads between 200 and 500nm [52]; consequently, the detection of NPs remains a challenge. Recently, dedicated small particle high-resolution flow cytometry (HRFCM) can offer a better resolution down to 40nm [53].

Cells and NPs are guided through a laser beam. The first detector is parallel to this beam and measures forward scattered light (FSC). The other detector is perpendicular to the beam and measures the side scattered light (SSC). FSC is used to look at the specimen size, whereas SSC is used to look at its granularity (Figure 8). The smaller the particle, the less the light scatters and the more background. FSC depends on the radius, the illumination wavelength, the refractive index and the light collection angle [54]. Thus, for an identical size, particles can have various refractive indices, resulting in a different scattering (Figure 9A). For the analysis of EVs, it is better to use silica beads for calibration, as EVs refractive index is closer to that of silica beads than polystyrene beads.

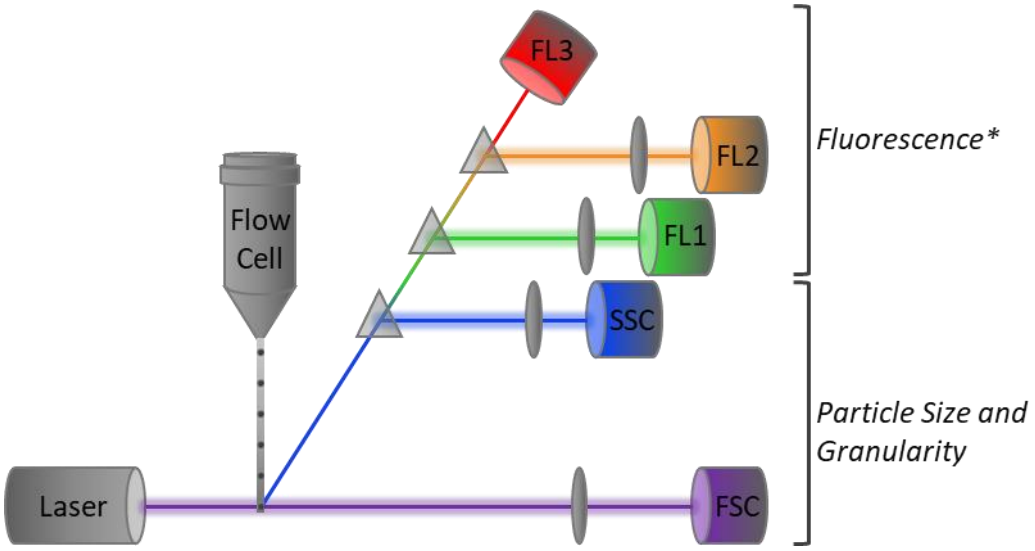

Figure 8 Schematic Representation of Particle Analysis by Flow Cytometry. *A particle suspension enters the flow cell where the particles are aligned into a single stream and pass through a focused laser-beam. The resultant signal provides information on their size/granularity based on their forward and side scatter and the fluorescent intensities (*if fluorescently labelled) of each particle.*

Fluorescent detection of surface proteins can also be achieved as long as the labelling of the NP is bright enough to discriminate NPs from the optical and electronic noise. To do so, the light scatter threshold can be modified, or the excess of label can be removed using a density gradient. Focusing on EVs, the fluorescence trigger can be used as long as the antigen is abundant enough to allow detection. This can be an issue for smaller particles with fewer copies of the antigen of interest [55]. Thus, sensitivity limits should be kept in mind when using fluorescently-labelled antibodies.

The concentration of the particles can have an important impact on both scatter and fluorescence [56]. If the concentration is too high, it will result in a swarm detection (Figure 9B). This occurs when two or more particles are in the measurement volume when the data acquisition is triggered, resulting in multiple NPs counted as a single event [57]. In order to have a better single NP detection, the samples need to be carefully diluted to an appropriate particle concentration. FCM offers a great possibility for single NP based analysis as long as there is a standardisation of the sample preparation as well as the appropriate instrument calibration.

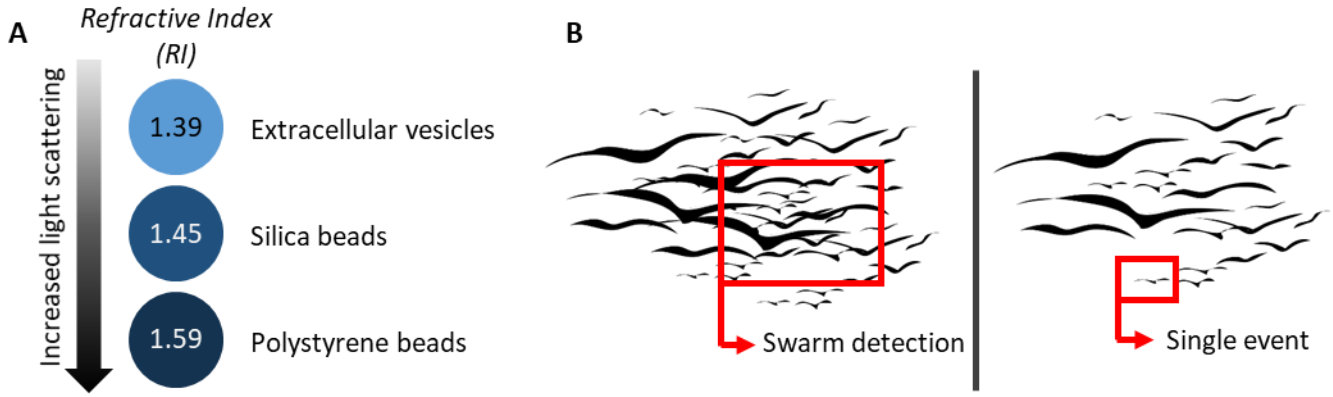

Figure 9 Principles of flow cytometry for NP analysis *A. Effect of the refractive index (RI) of different nature of nanoparticles on the light scattering. B. Representation of particle flowing: swarm detection in opposition to a single event detection. Individual seagull representing an individual particle.*

Tunable resistive pulse sensing (TRPS)

Tunable resistive pulse sensing (TRPS), previously known as scanning ion occlusion spectroscopy (SIOS) [58], is suitable for biological and inorganic NP size, concentration and charge analysis. The equipment most largely associated with TRPS is produced by Izon Science Ltd and can be referred to as qNano.

TRPS requires a nanosized stretchable pore that separates two conductive fluid compartments. After applying a voltage across the nanopore, a current is established which is disrupted by the movement of particles through the nanopore. When a particle moves through the opening, it decreases the flow of ions through the nanopore, causing a transient current decrease known as a blockade event [59]. The amplitude of this event provides information for the size profiling of the particle. The number of blockades throughout time gives information about the concentration (Figure 10). NP measurement using TRPS requires an initial run with a calibration sample of known diameter and concentration, usually polystyrene beads of a modal size appropriate to the range of interest [41,42]. Samples and calibration should ideally be performed in the same buffer, which can cause issues with biological samples. Spiking the sample directly with calibration beads offers an alternative calibration method.

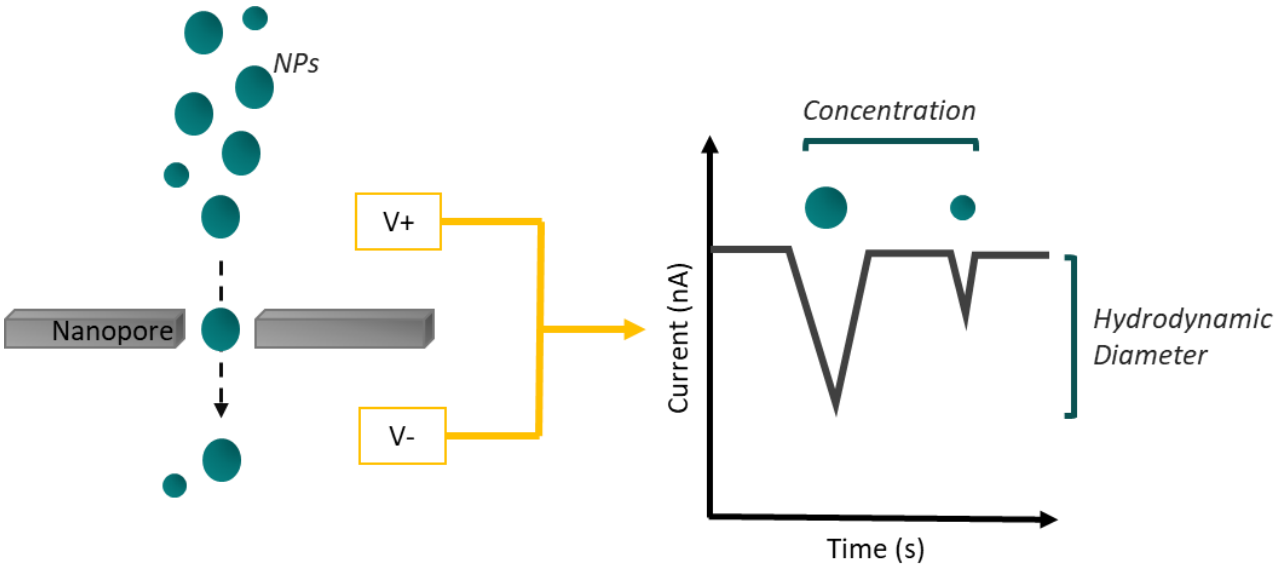

Figure 10 Principle of the TRPS technique to measure the diameter and concentration of nanoparticles. *The magnitude of the blockade event gives information on the hydrodynamic diameter, whereas the number of blockades over time gives information on the concentration.*

The size range of the nanopores can be tuned depending on the NPs of interest. Currently, the smallest nanopore is the NP100 that has a size range of 70-200nm. However, the full range of manufactured tunable pores extends from 70nm to 10µm. The measurement settings are flexible between each user. Different parameters can be adjusted in order to have the best measurement conditions, such as the nanopore stretch, the applied voltage and the pressure. The same parameters must be used between measurements to ensure the reproducibility of the data. A total of 500 particles or more is then counted per measurement. The TRPS technique provides a particle-by-particle analysis of the size and concentration using tunable nanopores. However, it can be challenging due to the size heterogeneity of the samples that can often lead to the blockage of the nanopore; this can be especially true for biological samples.

TECHNIQUE	ADVANTAGES	DISADVANTAGES
EM	High resolution Morphology 3D Contrast	Expensive equipment Specific training and expertise Radiation damage Sample preparation Invasive/destructive technique Highly time consuming
AFM	Atomic resolution Morphology/ surface roughness Sample preparation	Expensive equipment Specific training and expertise Highly time consuming
DLS	Quick Easy to use Relatively inexpensive High throughput	Low resolution in polydisperse samples Tendency to oversize particles due to Rayleigh's approximation of scattered light
NTA	Quick Easy to use Relatively inexpensive High throughput	Data bias dependent on user settings Dependent on refractive index Low resolution in highly concentrated polydisperse samples due to Rayleigh's approximation. Moderately time consuming
FCM	Full NP diameter range High throughput Multiparametric analysis	Low resolution Risk of swarm detection Low sensitivity no information about morphology Moderately time consuming
TRPS	Inexpensive Reusable pore Single particle-based analysis High throughput	Easily clogged nanopores Calibration required Moderately time consuming Required standardisation

Table 1 Comparison of the conventional techniques used to characterize the size and concentration of NPs.

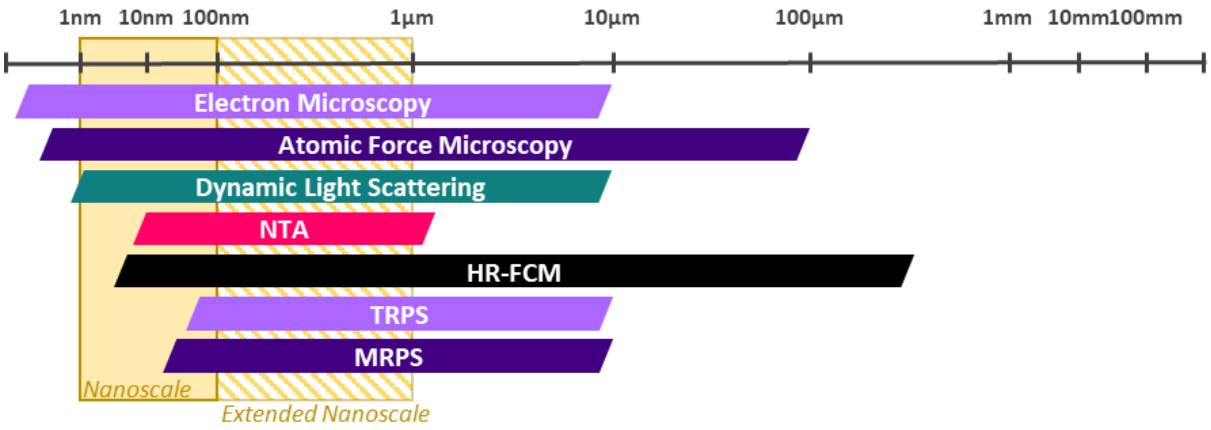

Figure 11 Size ranges for particle analysis of discussed techniques.

Each technique for NP characterisation has different limitations and advantages (Table 1 and Figure 11) [62]. Thus, it is often recommended to combine several techniques instead of choosing one method, as there is no standard procedure for the characterisation of NPs to date.

Recent Advances in Nanoparticle Analysis

Microfluidic resistive pulse sensing

Microfluidic resistive pulse sensing (MRPS) is a promising advancement in the resistive pulse sensing techniques originally described in the Coulter Principle over half a century ago [63]. The last decade has seen advancement in the form of TRPS (see the previous section). Although TRPS has pushed the limits of size detection of the resistive pulse sensing (RPS) technique, it still has limitations which need to be addressed for research to progress. In recent years there has been rapid development in the manufacturing of microfluidic chips and devices. An American company, Spectradyne, has utilised this research to develop an RPS instrument with patented microfluidic technology, the nCS1 [64].

The microfluidic technology in question is a series of pre-calibrated, single-use, low volume microfluidic cartridges. Each cartridge has a distinct size and concentration range (Figure 12). This has the benefits of making the technique an absolute method, i.e. no need for calibration material, the disposable microfluidic cartridges also dramatically reduce the risk of sample cross-contamination, with the added advantage of only requiring 3µL of sample to gain reliable, reproducible, statistically significant results.

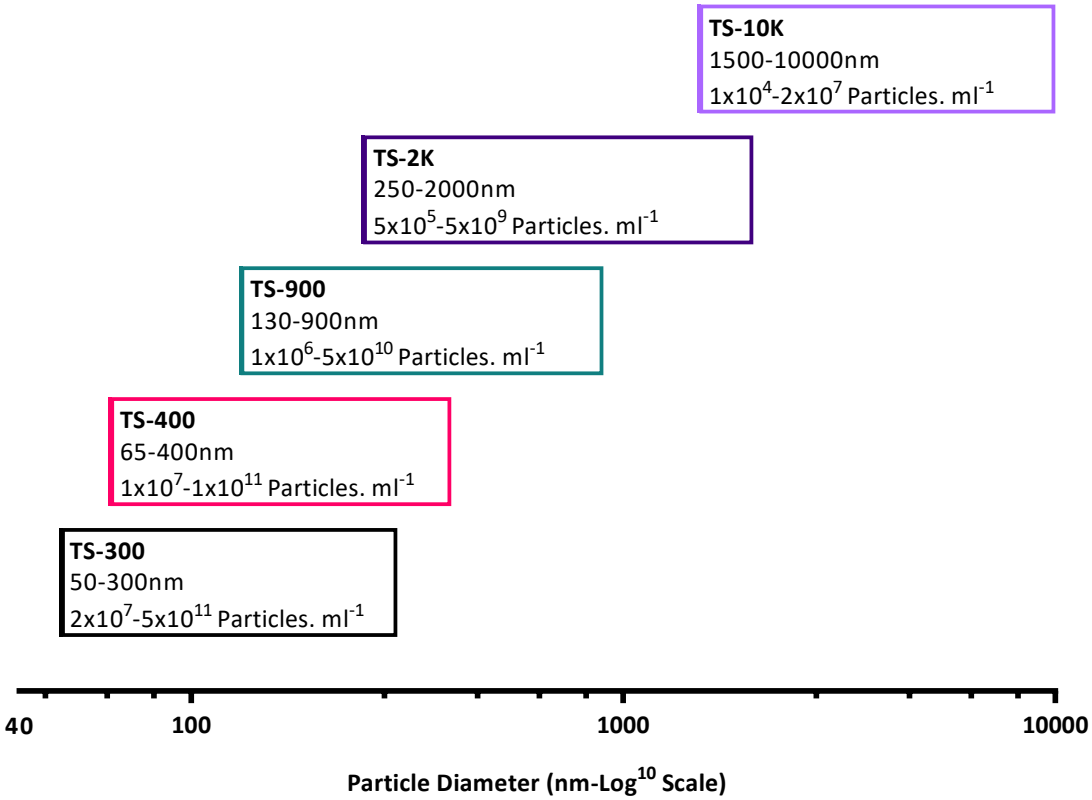

Figure 12 nCS1 Cartridge map denoting the size and concertation ranges.

The principle of the technique is essentially the same as that described by Wallace Coulter [63], whereby, a voltage is applied across an aperture (hole) submerged in an electrolyte, as a particle passes through the aperture (also termed a nano-constriction) the displacement of the electrolyte causes a voltage drop which is proportional to the size/volume of the particle, enabling its hydrodynamic diameter to be calculated [63],[65],[66]. This allows the user to obtain analytical data for individual particles making the technique highly precise.

The microfluidic cartridge of Spectradyne's nCS1 also significantly reduces one of the major issues of the RPS technique, which is aperture blockages by incorporating a sample pre-filter embedded within the microfluidic cartridge. The only drawback with the incorporation of this pre-filter is overcoming the surface tension in the smallest (TS-300/-400) size cartridges. Spectradyne recommends the addition of a surfactant (polysorbate-20/ Tween-20) at 1%(v/v) to the sample or 0.1%(w/v) bovine serum albumin (BSA) as a wetting agent where surfactant cannot be used (i.e. with lipidic samples).

The technology also overcomes some of the more technical aspects of the technique, such as distinguishing agglomerated particles from monodisperse particles. It does this in the form of filters applied to the data with parameters specific to each of the different sized cartridges, such as transit time, the time it takes the particle to pass through the aperture, and symmetry.

Analysis of nanoparticles using the nCS1

To test the capabilities of the instrument, a polydisperse sample of polystyrene size standards (Nanospheres) were analysed (Figure 13A). A broad range of Nanospheres were used (see Figure 13B) this was to test the accuracy of the instrument over multiple size cartridges. The Nanospheres were used at an approximate concentration of 4.2E+8 particles.mL^{-1}, i.e. a total concentration of 2.52E+9 particles.mL^{-1} in the polydisperse sample, this is in line with the acceptable concentration range for both the TS-400 and TS-2K cartridges used in the analysis. Approximately 2500 particles were analysed with default cartridge filters applied (Table S1); the subsequent data was analysed graphically by determining size ranges for Gaussian analysis/fit (Table S2).

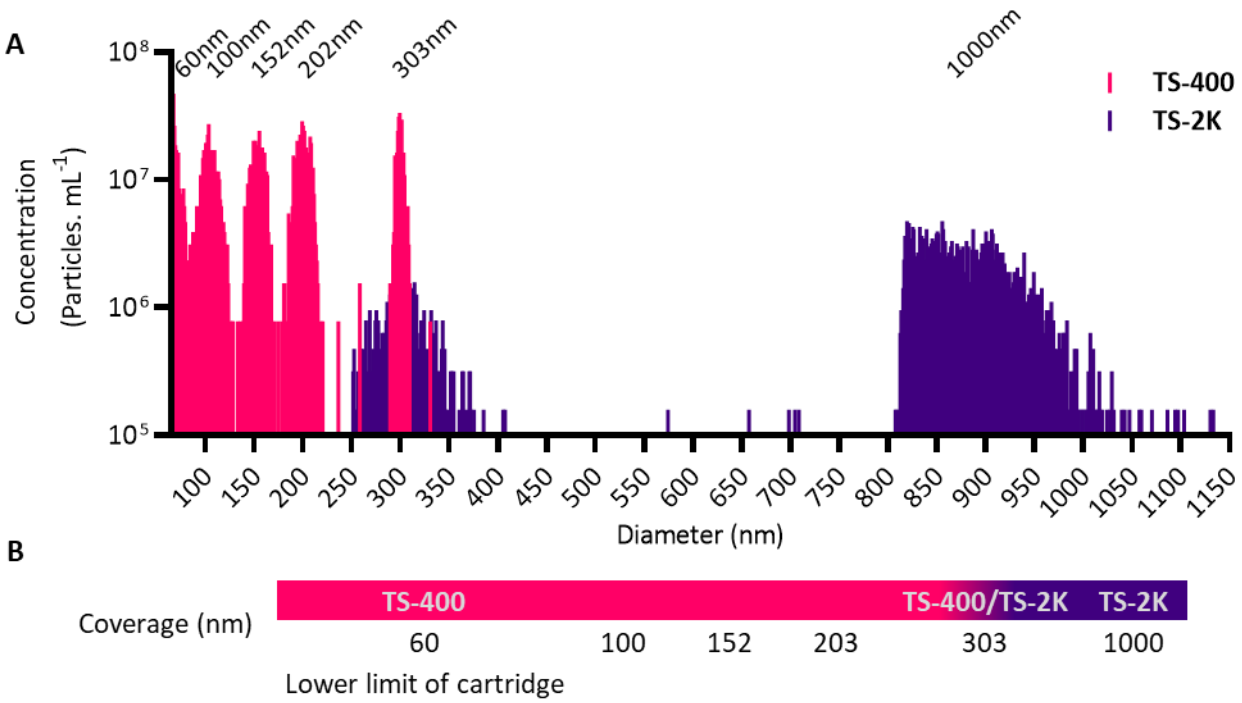

Figure 13 Analysis of a polydisperse polystyrene size standard sample using the nCS1. *A. Size distribution data demonstrating clear separation of peaks corresponding to the nominal size range of the polystyrene standards, the TS-2K cartridge perfectly overlays with the TS-400 cartridge at 303nm however demonstrates a broader distribution. B. Schematic demonstrates the size standards used in the polydisperse mix and the theoretical coverage of the cartridges.*

The data demonstrates that the nCS1 is capable of discerning multiple peaks in a single polydisperse sample. The TS-400 coverage range starts at 65nm; therefore, the resolution of the 60nm Nanosphere is hindered, resulting in a slight oversizing of the particle (Nanosphere™ NIST traceable certified diameter of 60±4nm), these data would be best captured using a TS-300 cartridge which has a lower detection threshold of 50nm. The other peak that demonstrated variability was the 1000nm peak; this showed a broad peak with a mean of 873.3nm (Figure 13, Table S1). The remaining discernible peaks fall within their certified mean diameter (provided on the safety data sheet), demonstrating the accuracy/resolution of the nCS1.

Analysis of Extracellular vesicles using the nCS1

Following analysis of the polystyrene size standards, we sought to test the instrument's capabilities at detecting a biological sample. Extracellular vesicles derived from apoptotic Jurkat cells were analysed for both size range and concentration. The apoptotic cell-derived EVs (ACdEVs) were isolated using centrifugation at 2000xg, and therefore it was suspected that the EVs could vary greatly in size; as such analysis using both a TS-300 and TS-900 was conducted. The analysis was conducted without the recommended surfactant (polysorbate-20) over concern that it could cause damage/ change the integrity of the EVs. Acquisition with the TS-900 demonstrated a continuous size distribution with a higher concentration of EVs at the lower size limit; this is in line with what was expected (

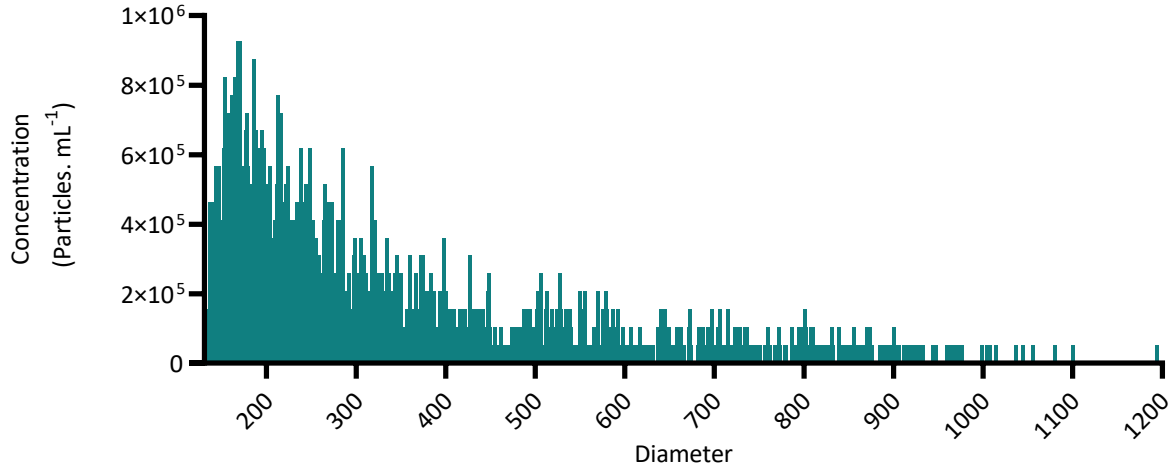

Figure **14**). Analysis across the entire TS-900 detection range (130-1000nm) reported a total of 2146 particles analysed in a time period of three minutes 30 seconds, demonstrating the high throughput capacity of the instrument. The concentration of particles across this range was calculated at 1.1E+08 particle.mL^{-1}, with a D10, D50, and D90 (corresponding to 10%, 50%, and 90% of particles in the concentration size distribution (CSD), see

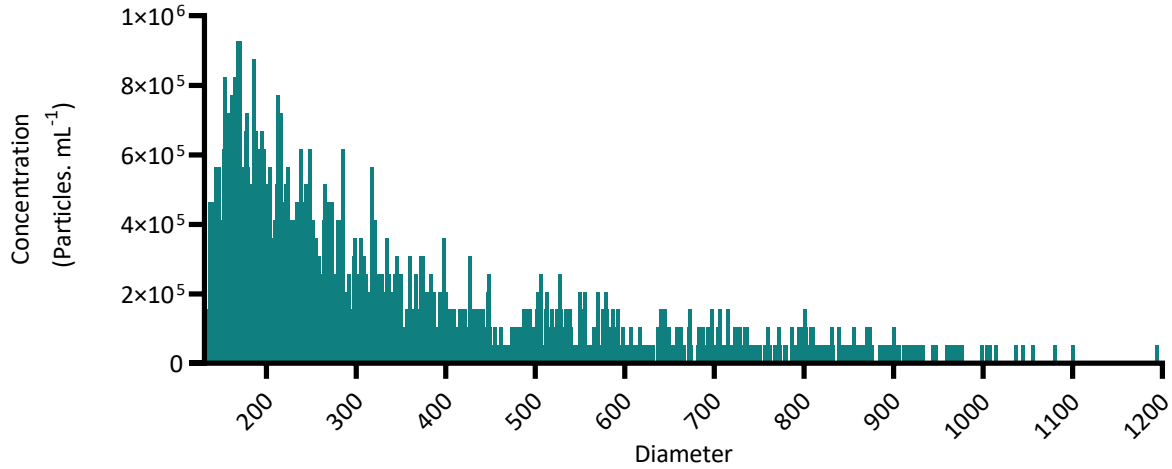

Figure **14** for CSD) of 164.8, 269.2, and 669.4nm respectively.

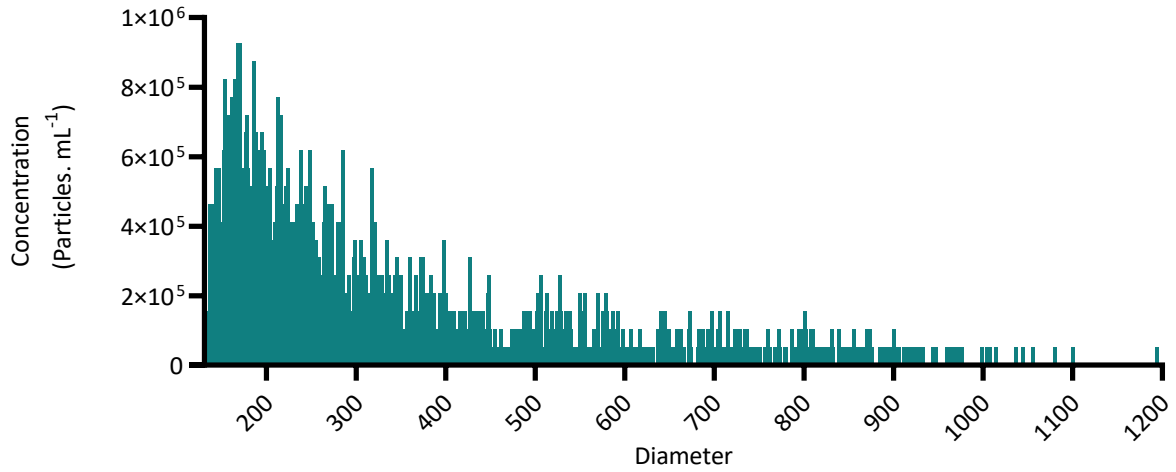

Figure 14 ACdEV analysis using the nCS1. *3µl of ACdEVs (Jurkat cells) in phenol-red free RPMI-1645 were analysed using a TS-900 cartridge on the nCS1. Approximately 2000 events/particles were analysed and demonstrate a size distribution with a higher concentration of EVs at the lower detection threshold.*

ACdEV analysis using the TS-300 cartridge was relatively unsuccessful with only a few (<100) discernible particles (data not shown). This did not acquire enough data for confident reporting of the size distribution. The lack of apparent particulate is surmised to be due to one of two reasons; the lack of surfactant in the sample and therefore a lack of wetting agent for the cartridge prefilter, or, the sheer concentration of particles/EVs larger than the aperture being retained in the prefilter and saturating it, and therefore severely reducing the flow of smaller particles. These hypotheses form part of ongoing investigations to identify an alternative to detergent as a wetting agent and to determine if pre-filtering for broad distributions is required. Nevertheless, MRPS shows great promise for the analysis of lipidic nanoparticles.

Conclusions

There are a wide variety of techniques for studying the size and concentration of lipidic NPs. Each approach has advantages and disadvantages, so careful thought is required to determine the correct technique for a particular sample. This is particularly true when a sample is highly polydisperse and may even contain particles outside of the nano range. This article illustrates the benefits and drawbacks of the most commonly-used approaches for analysing NPs and highlights the promising new technique of MRPS. It is nearly always advantageous to apply multiple approaches to a particular sample to enable the most complete analysis to be performed.

Material and methods

Cell lines and culture

Jurkat T cell line, derived from an acute T cell leukaemia patient, were cultured at a density of 5E+05 cells.mL^{-1} in RPMI 1640 medium (Sigma, Aldrich, UK) supplemented with 10% (v/v) FBS, 100 µg.mL^{-1} penicillin/streptomycin, and 2mM glutamine. Cells were passaged every two to three days and maintained at 37°C, 5% v/v CO_2.

EVs production

Jurkat cells were washed with PBS and resuspended in serum-free and phenol red-free RPMI-1640 (Sigma, Aldrich, UK) at a density of 4E+06 cells.mL^{-1}. Cells were then irradiated with a UV-B dose of 30

mJ.$(cm^2)^{-1}$ using the UVP chromato-vue C71 cabinet. Analysis of apoptosis was performed using annexin V-FITC / propidium iodide (PI) staining kit (BioLegend, San Diego) to confirm the cell death by flow cytometry (CytoFLEX S, Beckman Coulter, USA).

Measurement on nCS1

- **Nanosphere analysis**

National Institute of Standards and Technology (NIST) traceable Nanosphere™ size standards (ThermoScientific) were suspended in Isoton-II solution with 1% Tween-20, filtered to 0.22 µm using a PES syringe filter, to create a polydisperse mixture (60, 100, 202, 303, and 1000nm) with a final concentration of ~2.52E+09 particles.mL^{-1}. 3µL of sample was loaded into two different cartridges, TS-400 and TS-2K, in order to visualize the different sized nanospheres.

- **ACdEV analysis**

3µL of ACdEVs suspended in phenol-red free RPMI (Sigma, Aldrich, UK) was loaded into TS-300 and TS-900 cartridges and loaded into the machine for analysis.

The cartridge mould I.D. and date has to be inserted into the software, this provides the auto analysis engine with the parameters of the cartridge loaded, the machine then automatically primes the cartridge and collects the data. The machine will collect and analyse 10-second analysis windows until you either manually stop the runs or enter stop acquisition parameters, such as number of particles, in the auto-analysis run window.

ACKNOWLEDGEMENTS

We are grateful for funding from the European Union's Horizon 2020 research and innovation programme under Marie Sklodowska-Curie grant agreement No 847419 (MemTrain) and from Innovate UK in the form of a Knowledge Transfer Partnership between Aston University and Meritics Ltd (KTP 11605).

REFERENCES

[1] ISO/TS 80004-2:2015(en), Nanotechnologies — Vocabulary — Part 2: Nano-objects. https://www.iso.org/obp/ui/#iso:std:iso:ts:80004:-2:ed-1:v1:en.

[2] Wolf P. The nature and significance of platelet products in human plasma. *Br J Haematol*. 1967. DOI:10.1111/j.1365-2141.1967.tb08741.x

[3] Gyorgy B, Szabo TG, Pasztoi M, et al. Membrane vesicles, current state-of-the-art: emerging role of extracellular vesicles. *Cell Mol Life Sci*. 2011;68(16):2667-2688. DOI:10.1007/s00018-011-0689-3

[4] Atkin-Smith GK, Tixeira R, Paone S, et al. A novel mechanism of generating extracellular vesicles during apoptosis via a beads-on-a-string membrane structure. *Nat Commun*. 2015;6:7439. DOI:10.1038/ncomms8439

[5] Zaborowski MP, Balaj L, Breakefield XO, Lai CP. Extracellular Vesicles: Composition, Biological Relevance, and Methods of Study. *Bioscience*. 2015;65(8):783-797. DOI:10.1093/biosci/biv084

[6] Caruso S, Poon IKH. Apoptotic cell-derived extracellular vesicles: More than just debris. *Front Immunol*. 2018;9(JUN). DOI:10.3389/fimmu.2018.01486

[7] Nieuwland R, Sturk A. Why do cells release vesicles? *Thromb Res*. 2010;125 Suppl:S49-51. DOI:10.1016/j.thromres.2010.01.037

[8] Lotvall J, Hill AF, Hochberg F, et al. Minimal experimental requirements for definition of extracellular vesicles and their functions: a position statement from the International Society for Extracellular Vesicles. *J Extracell Vesicles*. 2014;3:26913. DOI:10.3402/jev.v3.26913

[9] Bangham AD, Horne RW. Negative staining of phospholipids and their structural modification by surface-active agents as observed in the electron microscope. *J Mol Biol*. 1964. DOI:10.1016/S0022-2836(64)80115-7

[10] Akbarzadeh A, Rezaei-Sadabady R, Davaran S, et al. Liposome: classification, preparation, and applications. *Nanoscale Res Lett*. 2013;8(1):102. DOI:10.1186/1556-276X-8-102

[11] Zhang X, Zhang P. Polymersomes in Nanomedicine - A Review. *Curr Nanosci*. 2016. DOI:10.2174/1573413712666161018144519

[12] Melis Çağdaş ADS and SB. Liposomes as Potential Drug Carrier Systems for Drug Delivery. In: *Application of Nanotechnology in Drug Delivery*. Ali Demir. IntechOpen. DOI:10.5772/58459

[13] Patel GB, Agnew BJ, Deschatelets L, Fleming LP, Sprott GD. In vitro assessment of archaeosome stability for developing oral delivery systems. *Int J Pharm*. 2000;194(1):39-49. DOI:10.1016/s0378-5173(99)00331-2

[14] Kaneda Y. Virosomes: evolution of the liposome as a targeted drug delivery system. *Adv Drug Deliv Rev*. 2000;43(2-3):197-205. DOI:10.1016/s0169-409x(00)00069-7

[15] Anupama Singh RM and PKS. Novasome-A Breakthrough in Pharmaceutical Technology a Review Article. *Adv Biol Res (Rennes)*. 2011;5(4):5.

[16] Hofheinz RD, Gnad-Vogt SU, Beyer U, Hochhaus A. Liposomal encapsulated anti-cancer drugs. *Anticancer Drugs*. 2005;16(7):691-707. DOI:10.1097/01.cad.0000167902.53039.5a

[17] Gill SE, Savage K, Wysham WZ, Blackhurst DW, Winter WE, Puls LE. Continuing routine cardiac surveillance in long-term use of pegylated liposomal doxorubicin: Is it necessary? *Gynecol*

Oncol. 2013;129(3):544-547. DOI:10.1016/j.ygyno.2013.03.012

[18] Sercombe L, Veerati T, Moheimani F, Wu SY, Sood AK, Hua S. Advances and Challenges of Liposome Assisted Drug Delivery. *Front Pharmacol*. 2015;6:286. DOI:10.3389/fphar.2015.00286

[19] van Rooijen N, van Nieuwmegen R. Liposomes in immunology: Multilamellar phosphatidylcholine liposomes as a simple, biodegradable and harmless adjuvant without any immunogenic activity of its own. *Immunol Invest*. 1980;9(3):243-256. DOI:10.3109/08820138009065997

[20] Bangham AD, Hill MW, Miller NGA. Preparation and Use of Liposomes as Models of Biological Membranes. In: *Methods in Membrane Biology*. ; 1974. DOI:10.1007/978-1-4615-7422-4_1

[21] Routledge SJ, Linney JA, Goddard AD. Liposomes as models for membrane integrity. *Biochem Soc Trans*. 2019;47(3):919-932. DOI:10.1042/BST20190123

[22] Wright J, Muench SP, Goldman A, Baker A. Substrate polyspecificity and conformational relevance in ABC transporters: New insights from structural studies. *Biochem Soc Trans*. 2018;46(6):1475-1484. DOI:10.1042/BST20180146

[23] Bayburt TH, Grinkova Y V., Sligar SG. Self-Assembly of Discoidal Phospholipid Bilayer Nanoparticles with Membrane Scaffold Proteins. *Nano Lett*. 2002;2(8):853-856. DOI:10.1021/nl025623k

[24] Bayburt TH, Grinkova Y V., Sligar SG. Self-Assembly of Discoidal Phospholipid Bilayer Nanoparticles with Membrane Scaffold Proteins. *Nano Lett*. 2002;2(8):853-856. DOI:10.1021/nl025623k

[25] Goddard AD, Dijkman PM, Adamson RJ, Dos Reis RI, Watts A. Reconstitution of Membrane Proteins: A GPCR as an Example. In: *Methods in Enzymology*. ; 2015. DOI:10.1016/bs.mie.2015.01.004

[26] Knowles TJ, Finka R, Smith C, Lin YP, Dafforn T, Overduin M. Membrane proteins solubilized intact in lipid containing nanoparticles bounded by styrene maleic acid copolymer. *J Am Chem Soc*. 2009;131(22):7484-7485. DOI:10.1021/ja810046q

[27] Clogston JD, Hackley VA, Prina-Mello A, Puri S, Sonzini S, Soo PL. Sizing up the Next Generation of Nanomedicines. *Pharm Res*. 2019;37(1):6. DOI:10.1007/s11095-019-2736-y

[28] Li P, Kaslan M, Lee SH, Yao J, Gao Z. Progress in exosome isolation techniques. *Theranostics*. 2017;7(3):789-804. DOI:10.7150/thno.18133

[29] Miranda K, Girard-Dias W, Attias M, de Souza W, Ramos I. Three dimensional reconstruction by electron microscopy in the life sciences: An introduction for cell and tissue biologists. *Mol Reprod Dev*. 2015. DOI:10.1002/mrd.22455

[30] Kisielowski C, Freitag B, Bischoff M, et al. Detection of single atoms and buried defects in three dimensions by aberration-corrected electron microscope with 0.5-Å information limit. *Microsc Microanal*. 2008. DOI:10.1017/S1431927608080902

[31] Matsumoto S, Ishida S, Araki M, Kato T, Terayama K, Okuno Y. Extraction of Protein Dynamics Information Hidden in Cryo-EM Map Using Deep Learning. February 2020:2020.02.17.951863. DOI:10.1101/2020.02.17.951863

[32] Stegmayr B, Brody I, Ronquist G. A biochemical and ultrastructural study on the endogenous protein kinase activity of secretory granule membranes of prostatic origin in human seminal plasma. *J Ultrastruct Res*. 1982;78(2):206-214. DOI:10.1016/s0022-5320(82)80024-5

[33] Efremov RG, Gatsogiannis C, Raunser S. Lipid Nanodiscs as a Tool for High-Resolution Structure Determination of Membrane Proteins by Single-Particle Cryo-EM. In: *Methods in Enzymology*. ; 2017. DOI:10.1016/bs.mie.2017.05.007

[34] Arraud N, Linares R, Tan S, et al. Extracellular vesicles from blood plasma: determination of their morphology, size, phenotype and concentration. *J Thromb Haemost*. 2014;12(5):614-627. DOI:10.1111/jth.12554

[35] Höög JL, Lötvall J. Diversity of extracellular vesicles in human ejaculates revealed by cryo-electron microscopy. *J Extracell Vesicles*. 2015;4(1):28680. DOI:10.3402/jev.v4.28680

[36] Midgley PA, Weyland M. 3D electron microscopy in the physical sciences: The development of Z-contrast and EFTEM tomography. In: *Ultramicroscopy*. ; 2003. DOI:10.1016/S0304-3991(03)00105-0

[37] Deng Y, Chen Y, Zhang Y, Wang S, Zhang F, Sun F. ICON: 3D reconstruction with 'missing-information' restoration in biological electron tomography. *J Struct Biol*. 2016. DOI:10.1016/j.jsb.2016.04.004

[38] Grubb DT. Radiation damage and electron microscopy of organic polymers. *J Mater Sci*. 1974;9(10):1715-1736. DOI:10.1007/BF00540772

[39] Binnig G, Quate CF, Gerber C. Atomic force microscope. *Phys Rev Lett*. 1986;56(9):930-933. DOI:10.1103/PhysRevLett.56.930

[40] Liu S, Wang Y. Application of AFM in microbiology: a review. *Scanning*. 2010;32(2):61-73. DOI:10.1002/sca.20173

[41] Martin Y, Williams CC, Wickramasinghe HK. Atomic force microscope-force mapping and profiling on a sub 100-Å scale. *J Appl Phys*. 1987;61(10):4723-4729. DOI:10.1063/1.338807

[42] Milhiet PE, Dosset P, Godefroy C, et al. Nanoscale topography of hepatitis B antigen particles by atomic force microscopy. *Biochimie*. 2011;93(2):254-259. DOI:10.1016/j.biochi.2010.09.018

[43] Dufrêne YF. Using nanotechniques to explore microbial surfaces. *Nat Rev Microbiol*. 2004;2(6):451-460. DOI:10.1038/nrmicro905

[44] Heath GR, Scheuring S. Advances in high-speed atomic force microscopy (HS-AFM) reveal dynamics of transmembrane channels and transporters. *Curr Opin Struct Biol*. 2019;57:93-102. DOI:10.1016/j.sbi.2019.02.008

[45] Humphris ADL, Antognozzi M, McMaster TJ, Miles MJ. Transverse dynamic force spectroscopy: A novel approach to determining the complex stiffness of a single molecule. 2002;18(5):1729-1733. DOI:10.1021/la015537k

[46] Anderson W, Kozak D, Coleman VA, Jämting ÅK, Trau M. A comparative study of submicron particle sizing platforms: Accuracy, precision and resolution analysis of polydisperse particle size distributions. *J Colloid Interface Sci*. 2013;405:322-330. DOI:10.1016/j.jcis.2013.02.030

[47] Finsy R. Particle sizing by quasi-elastic light scattering. *Adv Colloid Interface Sci*. 1994;52(C):79-143. DOI:10.1016/0001-8686(94)80041-3

[48] Gross J, Sayle S, Karow AR, Bakowsky U, Garidel P. Nanoparticle tracking analysis of particle size and concentration detection in suspensions of polymer and protein samples: Influence of experimental and data evaluation parameters. *Eur J Pharm Biopharm*. 2016;104:30-41. DOI:10.1016/j.ejpb.2016.04.013

[49] *Introduction to Nanoparticle Tracking Analysis (NTA) Measurement Principle of ZetaView®*. www.particle-metrix.de.

[50] NanoSight NS300 | Characterize Nanoparticles | Malvern Panalytical. https://www.malvernpanalytical.com/en/products/product-range/nanosight-range/nanosight-ns300.

[51] Wright M. Nanoparticle tracking analysis for the multiparameter characterization and counting of nanoparticle suspensions. *Methods Mol Biol*. 2012;906:511-524. DOI:10.1007/978-1-61779-953-2_41

[52] Steen HB. Flow cytometer for measurement of the light scattering of viral and other submicroscopic particles. *Cytom A*. 2004;57(2):94-99. DOI:10.1002/cyto.a.10115

[53] Saywell A, Bakker A, Mielke J, et al. Light-Induced Translation of Motorized Molecules on a Surface. *ACS Nano*. 2016;10(12):10945-10952. DOI:10.1021/acsnano.6b05650

[54] Welsh JA, Holloway JA, Wilkinson JS, Englyst NA. Extracellular Vesicle Flow Cytometry Analysis and Standardization. *Front Cell Dev Biol*. 2017;5:78. DOI:10.3389/fcell.2017.00078

[55] Nolan JP, Duggan E. Analysis of individual extracellular vesicles by flow cytometry. In: *Methods in Molecular Biology*. ; 2018. DOI:10.1007/978-1-4939-7346-0_5

[56] Groot Kormelink T, Arkesteijn GJ, Nauwelaers FA, van den Engh G, Nolte-'t Hoen EN, Wauben MH. Prerequisites for the analysis and sorting of extracellular vesicle subpopulations by high-resolution flow cytometry. *Cytom A*. 2016;89(2):135-147. DOI:10.1002/cyto.a.22644

[57] van der Pol E, van Gemert MJ, Sturk A, Nieuwland R, van Leeuwen TG. Single vs. swarm detection of microparticles and exosomes by flow cytometry. *J Thromb Haemost*. 2012;10(5):919-930. DOI:10.1111/j.1538-7836.2012.04683.x

[58] Roberts GS, Yu S, Zeng Q, et al. Tunable pores for measuring concentrations of synthetic and biological nanoparticle dispersions. 2012;31(1):17-25. DOI:10.1016/j.bios.2011.09.040

[59] Maas SL, Broekman ML, de Vrij J. Tunable Resistive Pulse Sensing for the Characterization of Extracellular Vesicles. *Methods Mol Biol*. 2017;1545:21-33. DOI:10.1007/978-1-4939-6728-5_2

[60] Vogel R, Willmott G, Kozak D, et al. Quantitative sizing of nano/microparticles with a tunable elastomeric pore sensor. *Anal Chem*. 2011;83(9):3499-3506. DOI:10.1021/ac200195n

[61] Maas SLN, Vrij J De, Broekman MLD. Quantification and size-profiling of extracellular vesicles using tunable resistive pulse sensing. *J Vis Exp*. 2014. DOI:10.3791/51623

[62] van der Pol E, Hoekstra AG, Sturk A, Otto C, van Leeuwen TG, Nieuwland R. Optical and non-optical methods for detection and characterization of microparticles and exosomes. *J Thromb Haemost*. 2010;8(12):2596-2607. DOI:10.1111/j.1538-7836.2010.04074.x

[63] Coulter WH. Means for counting particles suspended in a fluid. October 1953.

[64] Fraikin J-L, Teesalu T, Mckenney CM, Ruoslahti E, Cleland AN. A high-throughput label-free nanoparticle analyser. 2011. DOI:10.1038/NNANO.2011.24

[65] Rhyner MN. The coulter principle for analysis of subvisible particles in protein formulations. *AAPS J*. 2011;13(1):54-58. DOI:10.1208/s12248-010-9245-6

[66] Graham MD. The Coulter Principle: Foundation of an Industry. 2003. DOI:10.1016/S1535-5535(03)00023-6

628